SIMULATION OF HEAT TRANSFER THROUGH WOVEN FABRICS BASED ON THE FABRIC GEOMETRY MODEL

by

Zhenrong ZHENG[a,b*], Nannan ZHANG[a], and Xiaoming ZHAO[a]

[a] College of Textiles, Tianjin Polytechnic University, Tianjin, China
[b] Key Laboratory of Advanced Textile Composites of Ministry of Education, Tianjin, China

Original scientific paper
https://doi.org/10.2298/TSCI160507128Z

Numerical simulation is a rapid, effective, and low cost method to predict the heat transfer performance of fabrics. However, in previous research fabrics are usually assumed to be a uniform plate. Here, geometry models of 5/3 satin weave, double plain weave, and double twill glass fiber fabrics have been established based on the fabric thickness, yarn path and yarn cross-section shape. In the fabric unit, air occupies 60% to 80% by volume of the fabric unit. Therefore, the air in the fabric unit should be considered in the numerical simulation by finite element analysis. In this work, the fabric unit cells consisted of a yarn domain and an air domain. Based on the fabric unit cell model, the finite element method was used to predict the heat transfer through fabrics. The numerical temperature data are very close to the experiment data for glass fiber fabrics. Prediction results show that the temperature of 5/3 satin fabrics increase more rapidly than the double layer fabrics, and the heating rate of double twill fabric is lower than that for the double plain weave fabric, and they coincide well with the experiment data.

Key words: *fabric geometry model, heat transfer, finite element method*

Introduction

Glass fiber fabrics have characteristics of softness, light weight, high intensity, non-combustion, thermal insulation, chemical stability, and can be easily shaped. They have an important application in the field of facility protection [1, 2]. To develop a thermal protective fabric, the current methods are experimental, the processing of which includes design of the fabric, weaving and testing at high temperatures. This method has lots of problems, such as long processing time, high cost, high energy consumption, and production of fumes. The numerical simulation of the heat transfer through fabrics can provide the theoretical basis for the design and application of the thermal protective fabric. It can be widely used in the design of thermal fabrics for firefighters, welder, hot pipelines, oil refining equipment, and so on.

Many researchers have tried different techniques to predict the thermal property of woven fabric. Wan and Fan [3] and Fan *et al.* [4] used the finite control volume method to predict heat transfer through fibrous assemblies incorporating reflective interlayers. Sun *et al.* [5] studied heat transfer through layers of textiles using the finite element method. Gong *et al*. [6] established the 1-D fabric heat transfer model, and ANSYS software was used to simulate and forecast the time of the second-degree burn injury of fabric samples. Wang *et al*. [7-9] proposed a much more efficient thermal lattice Boltzmann algorithm to predict the effective

* Corresponding author, e-mail: tianjinzhengzr@163.com

thermal conductivity of various materials, such as complex multiphase materials, composites and fibrous materials. They found it was useful for design and optimization of new materials, beyond just predicting and analyzing the existing ones. Chen *at al.* [10] used the finite element simulation to predict the response of different layers of fabric to investigate the ballistic performance of hybrid fabric panels. Tian *et al*. [11] investigated the effects of layering sequence on the thermal response of multilayer fibrous materials under unsteady-state cases. It found that the fabric in contact with the hot heat source was the key layer to affecting the system's thermal response.

Woven fabrics are classified into weave or structure according to the style in which warp and weft cross each other. The texture of fabric has a significant effect on properties such as thermal insulation, mechanical behavior, and moisture permeability [12]. Some of the popular patterns for engineering purposes are plain, twill and satin weave [13]. Thermal behaviors of the fabric change if any of the weave patterns varies. Fabrics are highly porous materials consisting mainly of solid fiber and air void spaces. The porosity of most fabrics ranges from 60-80% [14, 15]. The effective thermal conductivity of the fabric with different fiber fractions was calculated by Muhammad *et al*. [16]. A computer-aided design (CAD) system for clothing thermal functional design and simulation was developed by Li *et al*. [17]. During the process of CAD system established, the porosity of the fabric was considered. Therefore, the air in the fabric unit should be considered in the numerical simulation.

In this paper, the glass fiber yarns were used to weave fabrics. A single yarn is made up of 1800 continuous filament fibers. The glass fiber yarn count is 280*tex* and 2 turns per cm. In order to smoothly create the fabric geometry model, the whole yarn is assumed as a pillar and the twist of yarn is not considered in the modeling process. Three structures of fabrics, 5/3 satin (12EPcm, 10PPcm), double plain (20EPcm, 10PPcm), and double twill (20EPcm, 10PPcm), were woven and used to model and simulate.

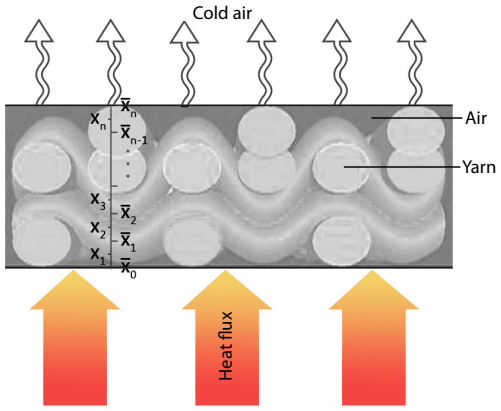

Figure 1. Schematic diagram of the glass fiber fabric

During the fabric geometry is modeled, the actual cross-sectional shape of the yarn, the rotation and deflection of yarns due to side-crimp forces are all considered. In this work, fabric geometry models have been established and the finite element method was used to predict the heat transfer through fabrics. The fabric geometry unit includes the yarn domain and the air domain, as shown in fig. 1.

Next, the heat transfer through the glass fiber fabrics have been investigated based on the fabric geometry model. The front faces of the fabrics were ablated using an alcohol blast burner at 900 °C, the verification experiment was done in the fume hood, so a convective heat transfer coefficient 15 W/m^2°C was defined on the back face of the fabric, shown in fig. 1. This research aims to identify and evaluate the heat transfer through fabrics, including details of temperature changes of the fabric through time, the temperature distribution at the cross-section of the fabric, the ambient temperature and the effects of fabric structure on the heat transfer properties. Furthermore, the experiments are used to validate the numerical simulation results.

Methodology

Geometrical modeling

Fabric geometric structures are determined mainly by the central paths and cross-sectional shapes of their constituent yarns. TexGen is an automated modelling approach [18]. It can easily describe the shape of yarn cross-section, yarn path and the yarn interweaving [19].

Yarn path representation

The path of a yarn can be considered as a 1-D line representing the yarn's center-line in 3-D space. The yarn path can be defined as its position in 3-D space as a function of distance along the yarn. To obtain an accurate yarn path for woven fabrics, it is sufficient to specify one or two master nodes per cross-over as long as the interpolation function is suitable. The most general form of yarn path is represented by a polynomial spline $S(t)$ (Bezier, natural or periodic cubic) [20]:

$$\mathrm{S}(t)=\begin{cases} S_0(t) & \text{if} \quad t_0 \le t \le t_1 \\ S_1(t) & \text{if} \quad t_1 \le t \le t_2 \\ \cdot & \\ \cdot & \\ \cdot & \\ \cdot & \\ S_{k-2}(t) & \text{if} \quad t_{k-2} \le t \le t_{k-1} \end{cases} \tag{1}$$

where t_i values S are called control nodes (knots). The vector $S = (S_0, S_1, \ldots, S_{k-2})$ is called a knot vector for the spline, shown in fig. 2.

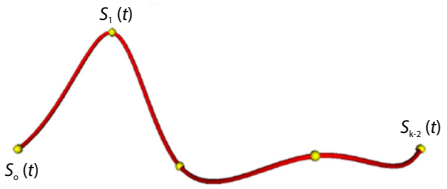

Figure 2. Periodic cubic splines

Yarn cross-section shape

The cross-section is defined as the 2-D shape of the yarn. Circular shape is one of the commonly used geometry models for yarn cross-section. However, the yarns are deflected duo to side crimp forces in the weaving process, generally yarn cross-sections are not circular [20]. Ellipse, power ellipse and lenticular shapes are other three types of geometry models for yarn cross-section.

Ellipse: It is a derivative of circular shape, and its equation is defined [20]:

$$\begin{aligned} C(t)_x &= \frac{w}{2}\cos(2\pi t) \\ C(t)_y &= \frac{h}{2}\sin(2\pi t) \end{aligned} \tag{2}$$

Yarn width, w, and height, h, were measured as the maximum distance between the yarn edges along the major and minor axes, respectively. As shown in fig. 3, yarn width is the distance of line AB, and yarn height is the distance of line CD. The $C(t)$ represents the knots of the ellipse, $C(t)x$ and $C(t)y$ are the x- and y- co-ordinates of the knots, respectively. If the distance of AB is equal to that of CD, the cross-section shape of yarn is a circle.

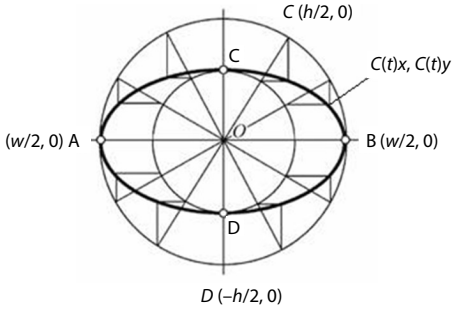

Figure 3. Ellipse cross-section

Power ellipse: The power ellipse is a slight modification to the elliptical cross-section where the y-coordinate is assigned a power n to make the section resemble a rectangle with rounded edges when $n < 1$ or a shape similar to a lenticular cross-section when $n > 1$. The power ellipse, is defined [20]:

$$C(t)_x = \frac{w}{2}\cos(2\pi t) \qquad 0 \le t \le 1$$
$$C(t)_y = \begin{cases} \frac{h}{2}\left[\sin(2\pi t)\right]^n & \text{if} \quad 0 \le t \le 0.5 \\ -\frac{h}{2}\left[-\sin(2\pi t)\right]^n & \text{if} \quad 0.5 \le t \le 1 \end{cases} \tag{3}$$

Lenticular: The lenticular cross-section is the intersection of two circles of radii r_1 and r_2 each offset vertically by distances O_1 and O_2, respectively. The parameters r_1, r_2, O_1, and O_2 can be calculated from the desired width, w, height, h, and distortion distance, d, of the lenticular section [20].

$$r_1 = \frac{w^2 + (h-2d)^2}{4(h-2d)}, \qquad r_2 = \frac{w^2 + (h+2d)^2}{4(h+2d)}, \qquad O_1 = -r_1 + \frac{h}{2}, \qquad O_2 = r_2 - \frac{h}{2} \tag{4}$$

Therefore, the lenticular section is described [20]:

$$C(t)_x = \begin{cases} r_1 \sin\theta & \text{if } 0 \le t \le 0.5 \\ r_2 \sin\theta & \text{if } 0.5 \le t \le 1 \end{cases}, \quad C(t)_y = \begin{cases} r_1 \cos\theta + O_1 & \text{if } 0 \le t \le 0.5 \\ -r_2 \cos\theta + O_2 & \text{if } 0.5 \le t \le 1 \end{cases} \tag{5}$$

where [19]:

$$\theta = \begin{cases} (1-4t)\sin^{-1}\frac{w}{2r_1} & \text{if} \quad 0 \le t \le 0.5 \\ (-3+4t)\sin^{-1}\frac{w}{2r_2} & \text{if} \quad 0.5 \le t \le 1 \end{cases} \tag{6}$$

Weave pattern

Woven fabrics are prepared by an interlacing arrangement between the warp and weft yarns. The weave pattern can be expressed by a 2-D binary matrix; 0 and 1 are used to represent the yarn interpenetrations. The 0 means the weft yarn over the warp yarn, and 1 means the warp yarn over the weft yarn. Figure 4 shows a binary array for a plain weave.

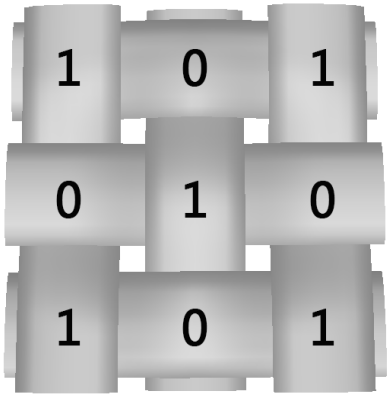

Figure 4. Plain weave

For 3-D weave patterns, since yarns interlace through multiple layers, the 2-D matrix method is limited. The 3-D fabric is defined by the centerlines of the yarn paths in 3-D space with superimposed cross-sections. The control nodes along a yarn path are created around a yarn circumference at interlacing points. These nodes help avoid yarn intersections and capture local waviness. Since an automated generator for 3-D fabric has been written by Python script in TexGen, the geometry models of orthogonal and angle inter-lock fabrics can be automatically generated. Some parameters, such as number of layers, yarn spacing (the dis-

tance from the edge of one yarn to the corresponding edge of an adjacent yarn), cross-sections of weft, warp and binder yarns, are required.

Geometric measurements

Fabric thickness was tested using YG141D digital fabric thickness gauge under area of pressing foot of 25 cm^2, pressing weight 20 CN/cm^2. The morphology of the satin weave and double plain weave fabrics was obtained by USB light microscopy (20X-400X, Dino-Lite, Taiwan, China). The morphology of the double twill weave fabric was obtained by SEM (TM1000, Hitachi, Japan). The cross-sectional images of the yarn were analyzed by imageJ software. The parameters (yarn spacing, width and height, cross-section shape) were measured and their values are shown in tab. 1. They were then used to create the unit cell geometries. Note that yarn spacing is the distance from the edge of one yarn to the corresponding edge of an adjacent yarn.

Table 1. Measured geometric dimensions for unit cell of glass fiber fabrics [mm]

Structure	Fabric thickness	Yarn width (warp/weft)	Yarn height (warp/weft)	Yarn spacing (warp/weft)	Yarn cross-section shape (warp/weft)
5/3 satin	0.90	0.60/0.62	0.42/0.46	0.64/0.80	ellipse/ellipse
Double plain	1.5	0.962/0.969	0.366-0.653/0.423-0.668	1.711/1.239	ellipse/ellipse
Double twill	1.457	1.096/1.004	0.490-0.627/0.538	1.56/1.224	ellipse/ellipse

Numerical solution with finite element method

Heat transfer equation

Heat transfer through a fabric system is a complex process, involving conduction, convection, and radiation processes. Considering the fabric thickness dimension is much smaller than the dimensions of fabric width and length, it is reasonable to assume the heat transfer through a fabric is a 1-D phenomenon. In this work, it is assumed that the thermal physical properties of fabrics and temperature of heat source were constant, the fabric boundary was adiabatic, and only conduction and convection heat transfers are considered and the radiative heat transfer is negligible. According to Fourier's law, Newton's law of cooling and energy conservation, the total heat flux is described:

$$Q_{\text{total}} = -\lambda A\frac{\mathrm{d}T(x)}{\mathrm{d}x} + Ah(T_\Gamma - T_\infty) \tag{7}$$

where $-\lambda A[\mathrm{d}T(x)/\mathrm{d}x]$ stands for the conduction heat flux, λ [$Wm^{-1}K^{-1}$] – the conductivity, A [m^2] – the heat flux area, T [K] – the temperature, x [m] – the direction of heat transfer, $Ah\,(T_\Gamma - T_\infty)$ stands for the convection heat flux, h [Wm^2K^{-1}] – the film coefficient, T_Γ [K] – the out surface temperature of the fabric, and T_∞ [K] – the temperature of the ambient atmosphere.

At the transient-heat condition, conduction heat transfer through the fabric in the thickness direction of the textile assembly is expressed [21-23]:

$$\frac{\partial T}{\partial t} = \frac{\lambda}{c\rho}\frac{\partial^2 T}{\partial x^2} \tag{8}$$

where T, t, λ, c, and ρ are temperature [K], time [s], conductivity [$Wm^{-1}K^{-1}$], specific heat [$JKg^{-1}K^{-1}$], and mass density [Kgm^{-3}] and x (m) represents the direction of heat transfer.

Since the fabrics consist of fibers and air, the fabric and air domains are defined, respectively, total conductive heat transfer area is divided into two parts, heat transfer through the zones of yarns and that of the air gaps. So it is reasonable that the physical parameters such as

the thermal conductivity, mass density, and specific heat of fabrics (λ_f, ρ_f, and c_f) and air (λ_g, ρ_g, and c_g) are assigned, respectively. The φ is the heat transfer area fraction of yarn, and 1-φ – the heat transfer area fraction of air-gap, which can be accurately obtained from the geometry model in ANSYS. Hence, the transient heat transfer of conduction heat is described:

$$\frac{\partial T}{\partial t} = \frac{\lambda_f \varphi}{c_f \rho_f} \frac{\partial^2 T_f}{\partial x_f^{\ 2}} + \frac{\lambda_g (1-\varphi)}{c_g \rho_g} \frac{\partial^2 T_g}{\partial x_g^{\ 2}} \tag{9}$$

Convection involves the transfer of heat energy in the air by movement of currents from high temperature fabric to the surroundings. When cold air moves past a warm fabric, it sweeps away warm air adjacent to the fabric and replaces it with cold air. Studies showed that there is no convection inside clothing insulation even with a very low density [24]. Hence, the convective heat transfer is considered only at the outer surface of the fabric. In the heat transfer analysis by ANSYS software, the convective heat transfer will be set as a boundary condition.

Substituting eq. (9) into eq. (7), we readily obtain the heat transfer equation at the transient heat condition:

$$\frac{\partial T}{\partial t} = \frac{\lambda_f \varphi}{c_f \rho_f} \frac{\partial^2 T_f}{\partial x_f^{\ 2}} + \frac{\lambda_g (1-\varphi)}{c_g \rho_g} \frac{\partial^2 T_g}{\partial x_g^{\ 2}} - h\left(\frac{T_\Gamma - T_\infty}{\partial x} \right) \tag{10}$$

Mesh generation and boundary conditions

The fabric models were converted to ANSYS workbench. Material properties were set as described in tab. 2. The specific heat and thermal conductivity of the fabrics were measured at 20 ºC by the hot disk thermal constant analyzer (TPS2500, Sweden). Here, the thermal conductivity of the fabric was tested in the thickness direction of the fabric.

Table 2. Physical parameters of the fabrics and air

Parameters	Thermal conductivity [$Wm^{-1}C^{-1}$]	Specific heat [$Jkg^{-1}C^{-1}$]	Fabric density [kgm^{-3}]
5/3 satin fabric	0.14	670	2400
Double plain fabric	0.074	1185.7	751.1
Double weave twill fabric	0.0585	1157.6	649.7
Air	0.0242	1006.4	1.225

Ten-node linear tetrahedral elements (SOLID 87) were used to mesh the unit cell, and the element edge length was all assigned as 0.2 mm. The automatic mesh generation was performed directly in these models. There were 32833 elements and 58656 nodes for the 5/3 satin fabric model, 80092 elements and 130680 nodes for the double plain weave fabric model, and 90889 elements and 147866 nodes for the double twill weave fabric model. The meshed unit cells of double plain weave fabric are shown in fig. 5.

Initial temperatures of fabric and environment are assigned as 22 °C. A temperature of 900 °C was loaded on the back face of the glass fiber fabric. The assumption is made that the experiment was done in the fume hood and the heat transfer between air and fabric is forced convection. The coefficient of convection heat transfer between air and fabric is 15 W/m^2 °C.

Numerical solution

The finite element method is used to compute the numerical solution of this integrative heat transfer mode. A positive integer N is selected. The $\overline{x} < \overline{x_1} < \overline{x_2} < ... \overline{x_N}$ is a discretization

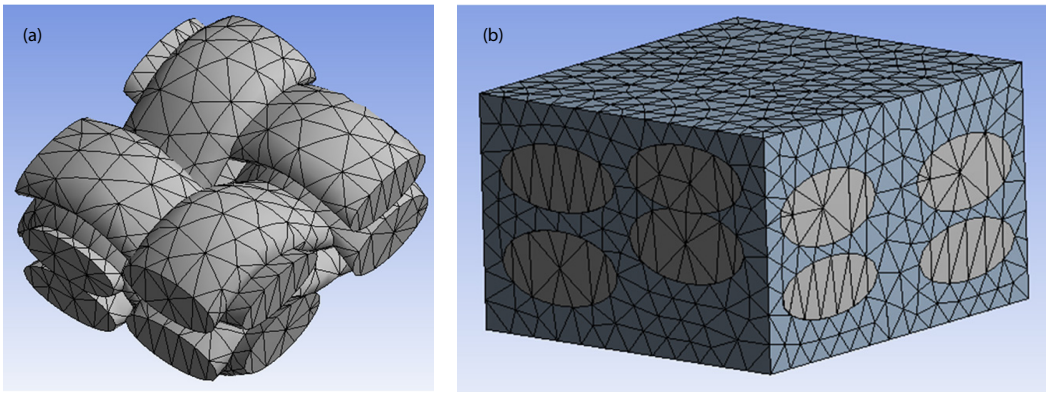

Figure 5. Meshed unit cell of double plain weave fabric; (a) without air fluid-matrix and (b) with air fluid-matrix

of fabric thickness and $[\overline{x}_{i-1}, \overline{x}_i]$ indicates the i^{th} control volume (shown in fig. 1). The grid points $x_1, x_2,..., x_N$ are located at the centers of control volumes, *i. e.*, $x_i = (\overline{x}_{i-2}, \overline{x}_i)/2$. The x_0, x_{N+1} are the two boundary points (they represent the points at the face and back side of the fabric, respectively). The distance between grid points is denoted by $\partial x_i = x_i - x_{i-1}$. Denote $T_i = T(x_i)$, $i = 0.1,...,$ $N+1$. If the value of temperature T_0 is obtained, the conductive heat and the total heat flow can be calculated by eq. (10). Hence, the value of temperature T_{N+1} can be calculated.

Verification of the model

Experiments have been carried out to validate the numerical simulation results. An illustration of the experimental process is shown in fig. 6. An asbestos gauze was placed above the flame, and a circle of radius 3 cm was cut out in its center. Then the fabric was placed on the asbestos gauze. The front face of the fabric was ablated using an alcohol blast burner at 900 ºC, and a convective heat transfer coefficient 15 W/m^2°C was defined for the back face of the fabric. An infrared thermocouple (Raytek, American) was used to measure the variation of the temperature of the back face of the fabric during the heating process. The lower the fabric temperature at the same heating time is, the better the heat resistance is.

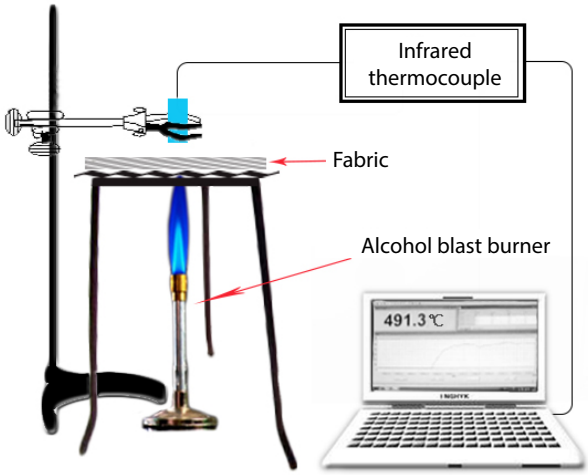

Figure 6. Illustration of the testing apparatus

Results and discussion

Geometry models

The fabric unit cell is described as the smallest unit of fabric structure. To simplify the fabric, the unit cells of fabrics are used for investigation by thermal transfer analysis. With the measured geometric dimension, the unit cells of glass fiber fabrics were created by using TexGen, and they are presented in figs. 7-9.

Figure 7(a) is the light microscopic image of 5/3 satin fabric, and fig. 7(b) shows its geometric model. The yarn paths of this fabric use the Bezier splines, and the weave pattern of the warp and weft yarns are the same as the real fabric. In figs. 7(c) and 7(d), the elliptical cross-sections are given to the warp yarn and weft yarn, respectively. Double layer fabric consists of two layers, which are woven one above the other. The generated model of double plain weave is shown in fig. 8. Ellipse cross-sections were assigned to the warp yarn and weft yarn. Figure 9 shows the geometry model of the double twill weave fabric. Compared with figs. 8(c) and fig. 8(d), the non-symmetrical structure of the twill weave gives bending and contact forces causing the yarns to rotate and deflect. As shown in fig. 9(c), the left yarns are rotated by 10º and the right yarns are rotated by –10º.

Simulation results and discussion

The simulation results of thermal distributions in the double plain fabric after 10 seconds are shown in fig. 10. Figure 10(a) shows the fabric unit cell with the air domain, and

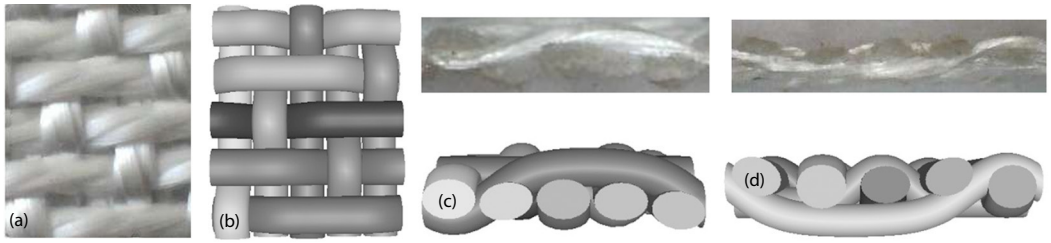

Figure 7. The 5/3 Satin fabric; microscopic image of (a) real fabric, (b) geometry model, (c) warp cross-section, and (d) weft cross-section

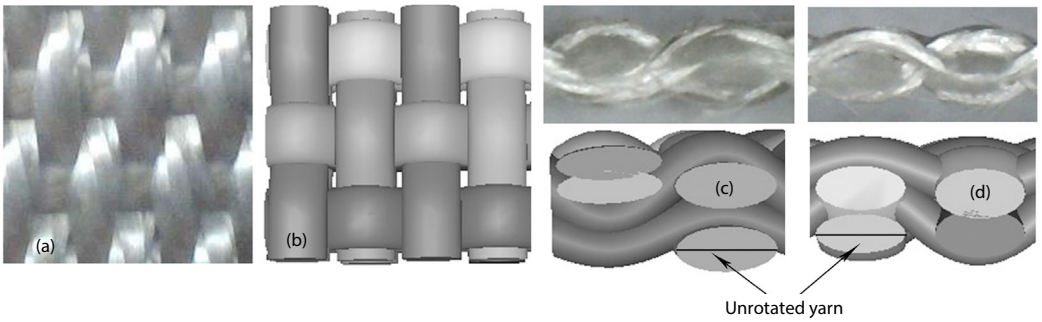

Figure 8. Double plain weave fabric; microscopic image of (a) real fabric, (b) geometry model, (c) warp cross-section, and (d) weft cross-section

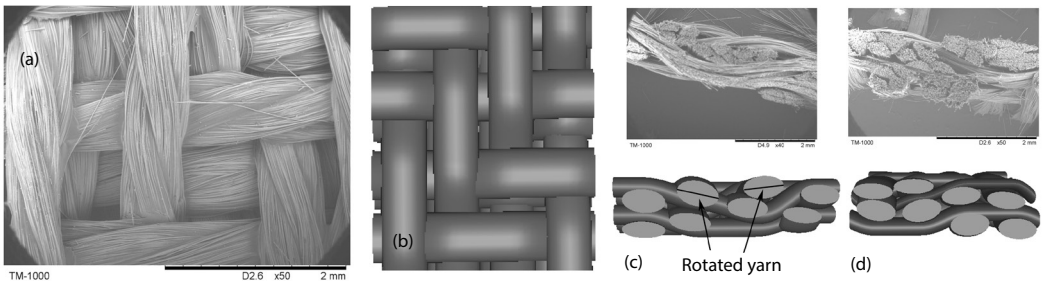

Figure 9. Double twill weave fabric; microscopic image of (a) real fabric, (b) geometry model, (c) warp cross-section, and (d) weft cross-section

the top face represents the heated face, which is subjected to a constant heat flux. The fabric cross-section shows the temperature gradually decreasing from the heated side of the fabric to the opposite side. Figure 10(b) shows the fabric only, where the air domain has been hidden. It is shown that the closer the fabric is to the heat source, the higher its temperature is. Figure 10(c) shows the heat distribution for the air domain, where the fabric part has been hidden.

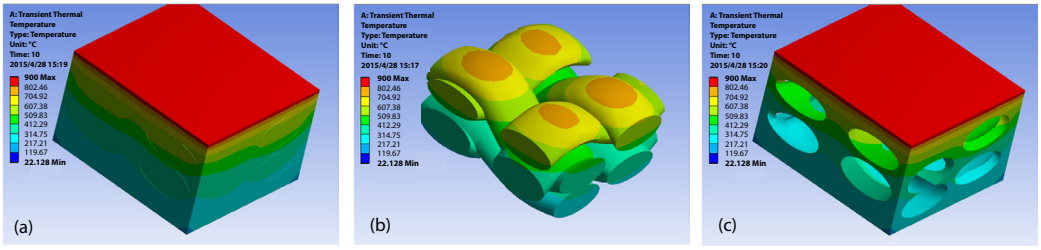

Figure 10. Heat flux distribution of double plain weave unit cell; (a) fabric with air domain, (b) fabric only, and (c) air domain only

The experimental temperatures of Nodes on the fabrics were compared with the numerical values from the finite element model. The results are shown in fig. 11. Figure 11(a) shows that the temperature in Node 1 of the satin fabric. The experimental temperature of the back face of the fabric rises rapidly, it reached 483 ºC in 5 seconds, then the temperature tends to stabilize. The numerical temperature data are very close to the experiment data, it indicates that the finite element model is able to predict the heat transfer property of the fabric.

Figure 11(b) shows that the experimental temperature of double plain weave rises to 307 ºC in 11 seconds and 453 ºC in 20 seconds. The numerical temperature was slightly higher than that for the experiment data. Figure 11(c) shows that the experimental temperature of the double twill fabric reached 299 ºC in 11 seconds and gradually reached 439 ºC in 20 seconds, and the numerical temperature was slightly lower than that for the experiment data. Correlation coefficients have been calculated for the experiment and numerical data for the satin weave, double plain and double twill weave fabrics, they were 0.995, 0.999, and 0.996, respectively. The average relative deviations at Node1, Node 2, and Node 3 were 8.1 %, 5.6 %, and 8 %, respectively. The thermophysical parameters of the fabric and air used in the simulation are the values measured at the standard temperature and humidity, which are constant in the heat transfer simulation process. However, the thermal conductivity, specific heat and density of the fabric and air change with the temperature increasing. It is necessary to further measure the thermophysical parameters at different temperatures, then the accuracy of the simulation will be improved.

The heat transfer properties of the satin fabric, the double plain weave and double twill fabrics were numerical and compared in fig. 11(d). It clearly shows that the temperature of the satin fabric increases more rapidly than the others, and the heating rate of the double twill fabric is lower than that for the double plain fabric. This is because the satin fabric is a single layer fabric, and the fabric thickness is less than the double-layer fabric. The double-layer fabrics have more yarns to defend the heat flux, and they can hold more still air within the fabric. Therefore, the double-layer fabrics have better thermal resistance. Compared with the double plain weave, the double twill fabric has less interlacing in the same area. It has more space to accommodate the still air, hence the temperature is lower after the same heating time. In fig. 11(d), the numerical models were successfully used to predict the heat transfer property of fabric, and the numerical results have excellent correlation with the experiment data.

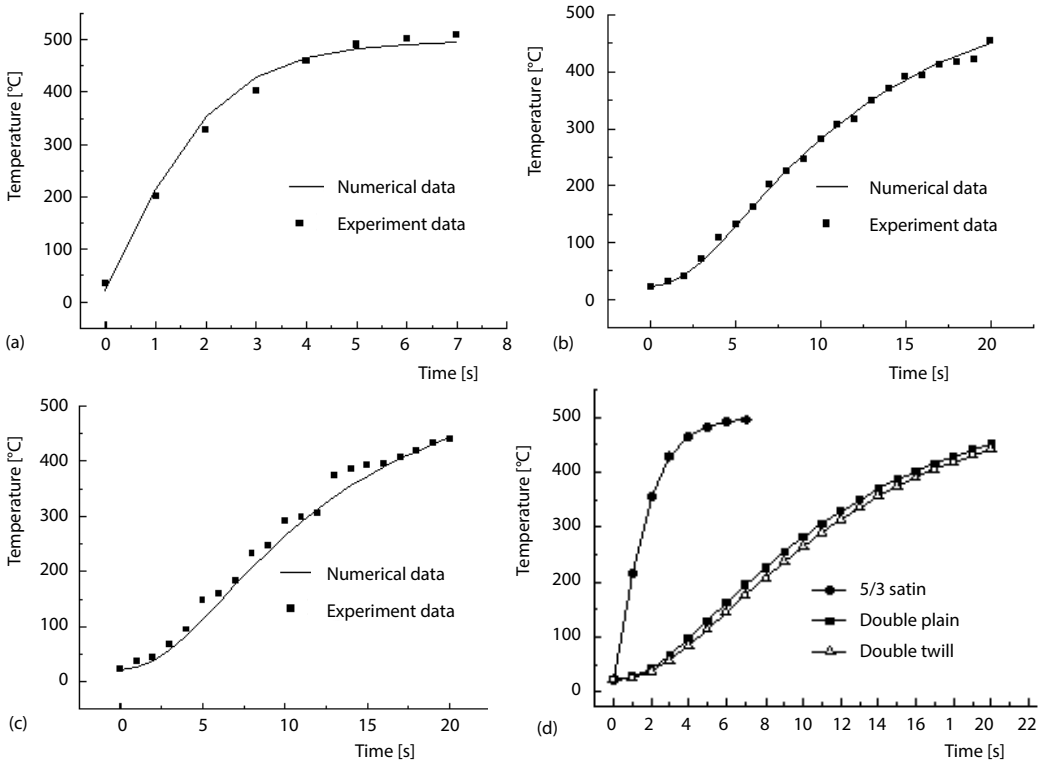

Figure 11. Experimental *vs.* numerical temperature data for the fabrics; (a) temperature in Node 1 of the satin fabric, (b) temperature in Node 2 of the double plain fabric, (c) temperature in Node 3 of the double twill fabric, and (d) comparison of temperature data for the three fabrics

Conclusions

The numerical simulation is a rapid, effective and low cost method to predict the heat transfer property of fabric. Normally, fabrics have been assumed to be a uniform plate. Woven fabrics are comprised of yarns, which are woven in one of several different patterns. Besides fibers and yarns in the fabric unit, lots of air holes exist and air occupies 60% to 80% by volume of the fabric unit. Therefore, the air in the fabric unit should be considered in the numerical simulation by finite element analysis. In this work, fabric geometry models have been established and the finite element method was used to predict the heat transfer through fabrics. The following conclusions can be made.

- Based on the fabric thickness, yarn path and yarn cross-section shape, the geometry models of 5/3 satin, double plain and double twill glass fiber fabrics have been established. The fabric unit cells consist of a yarn domain and an air domain, and the fabric geometry models are very close to the real fabrics.
- The numerical temperatures are very close to the experimental temperatures for the glass fiber fabrics, it indicated that the finite element model is able to predict the heat transfer property of the fabric.
- The temperature of the 5/3 satin fabric increases more rapidly than the double-layer fabrics, and the heating rate of the double twill fabric is lower than that for the double plain weave fabric.

Acknowledgment

This work was supported by the National Natural Science Foundation of China under Grant 51206122, Natural Science Foundation of Tianjin under Grant 13JCQNJC03000 and Technical Guidance Project of China National Textile and Apparel Council under Grant 2012002.

References

[1] Alongi, J., *et al*., Current Emerging Techniques to Impart Flame Retardancy to Fabrics: An Overview, *Polym. Degrad. Stab*., *106* (2014), Aug., pp.138-149
[2] Poon, C. K., *et al*., Effects of TiO_2 and Curing Temperatures on Flame Retardant Finishing of Cotton, *Carbohydr. Polym*., *121* (2015), May, pp. 457-467
[3] Wan, X., Fan, J. T., Heat Transfer through Fibrous Assemblies Incorporating Reflective Interlayers, *Int. J. Heat Mass Trans.*, *55* (2012), 25-26, pp. 8032-8037
[4] Fan, J. T., *et al*., Modeling Heat and Moisture Transfer through Fibrous Insulation with Phase Change and Mobile Condensates, *Int. J. Heat Mass Trans*., *45* (2002), 19, pp. 4045-4055
[5] Sun,Y., *et al*., Study of Heat Transfer through Layers of Textiles Using Finite Element Method, *Int*. J. *Cloth. Sci. and Tech*., *22* (2010), 2-3, pp. 161-173
[6] Gong, Y. R., *et al*., Numerical Simulation on Thermal Protection Properties of Textile Materials, *Journal of Donghua University* (*Natural Science*), *36* (2010), 1, pp. 115-117
[7] Wang, M. R., *et al.*, Lattice Boltzmann Modeling of the Effective Thermal Conductivity for Fibrous Materials, *Int. J. Therm. Sci*., *46* (2007), 9, pp. 848-855
[8] Wang, M. R., *et al*., Predictions of Effective Physical Properties of Complex Multiphase Materials, *Mater*. *Sci. Eng*. R, *63* (2008), 1, pp. 1-30
[9] Wang, M. R., *et al*., Thermal Conductivity Enhancement of Carbon Fiber Composites, *Appl. Therm. Eng*., *29* (2009), 2-3, pp. 418-421
[10] Chen, X. G., *et al*., Numerical and Experimental Investigations into Ballistic Performance of Hybrid Fabric Panels, *Composites Part B*, *58* (2014), Mar., pp. 35-42
[11] Tian, M. W., *et al*., Effects of Layering Sequence on Thermal Response of Multilayer Fibrous Materials: Unsteady-State Cases, *Therm. Fluid Sci*., *41* (2012), Sept., pp.143-148
[12] Cao, J., *et al*., Characterization of Mechanical Behavior of Woven Fabrics: Experimental Methods and Benchmark Results, *Composites Part A*, *39* (2008), 6, pp. 1037-1053
[13] Suppakul, P., *et al*., The Effect of Weave Pattern on the Mode-I Interlaminar Fracture Energy of E-glass Vinyl Ester Composites, *Compos. Sci. Technol*., *62* (2002), 5, pp. 709-717
[14] Wang, T., *et al*., Introduction to the Thermal and Humid Comfort and Evaluation Method, China Fiber Inspection, (2015), pp.74-76
[15] Zhang, C., Thermal Comfort and Climate in Clothing, *Journal of Wu Han University of Science and Engineering*, *18* (2005), pp. 4-7
[16] Muhammad, O. R. S., *et al*., Finite Element Analysis of Thermal Conductivity and Thermal Resistance Behavior of Woven Fabric, *Comput. Mater. Sci*., *75* (2013), July, pp. 45-51
[17] Li, Y., *et al*., P-Smart – A Virtual System for Clothing Thermal Functional Design, *Computer-Aided Design*, *38* (2006), 7, pp. 726-739
[18] Lin, H., *et al*., Finite Element Modelling of Fabric Compression, *Modelling Simul. Mater. Sci. Eng*., 16 (2008), 3, pp. 1-16
[19] Wong, C .C., *et al*., Comparisons of Novel and Efficient Approaches for Permeability Prediction Based on the Fabric Architecture, *Composites Part A*, *37* (2006), 6, pp. 847-857
[20] Sherburn, M., Geometric and Mechanical Modelling of Textiles, Ph. D. thesis, University of Nottingham, Nottingham, UK, 2007
[21] Farnworth, B., Mechanisms of Heat Transfer through Clothing Insulation, *Textile Res. J*., *53* (1983), 12, pp. 717-725
[22] Yang, S. M., *et al*., *Heat Transfer*, Higher Education Press, Beijing, 1999
[23] Incropera, F. P., *et al*., *Fundamentals of Heat Transfer*, 5th ed., Wiley Somerset, New York, USA, 2002
[24] Pierce, F. T., *et al*., The Transmission of Heat through Textile Fabrics – Part II, *Journal Text. Inst*., *37* (1946), 9, pp. 181-204

Paper submitted: May 7, 2016
Paper revised: May 10, 2017
Paper accepted: May 10, 2017